The space weather effects of the December 1, 2023 geomagnetic storm on GNSS PPP accuracy

Donghe Zhang, Yi Zeng, Ke LI
School of the Earth and Space Science, Peking University
zhangdh@pku.edu.cn

,Austria， 3–8 May 2026.

北京大学 PEKING UNIVERSITY

Outline

- Background and Motivation
- Data and method
- Morphological Variation of Ionospheric Irregularities/Scintillation from Different parameters during Storm
- Space Weather Effect on Carrier signal and Positioning Accuracy
- Discussion and Summary

Background and Motivation

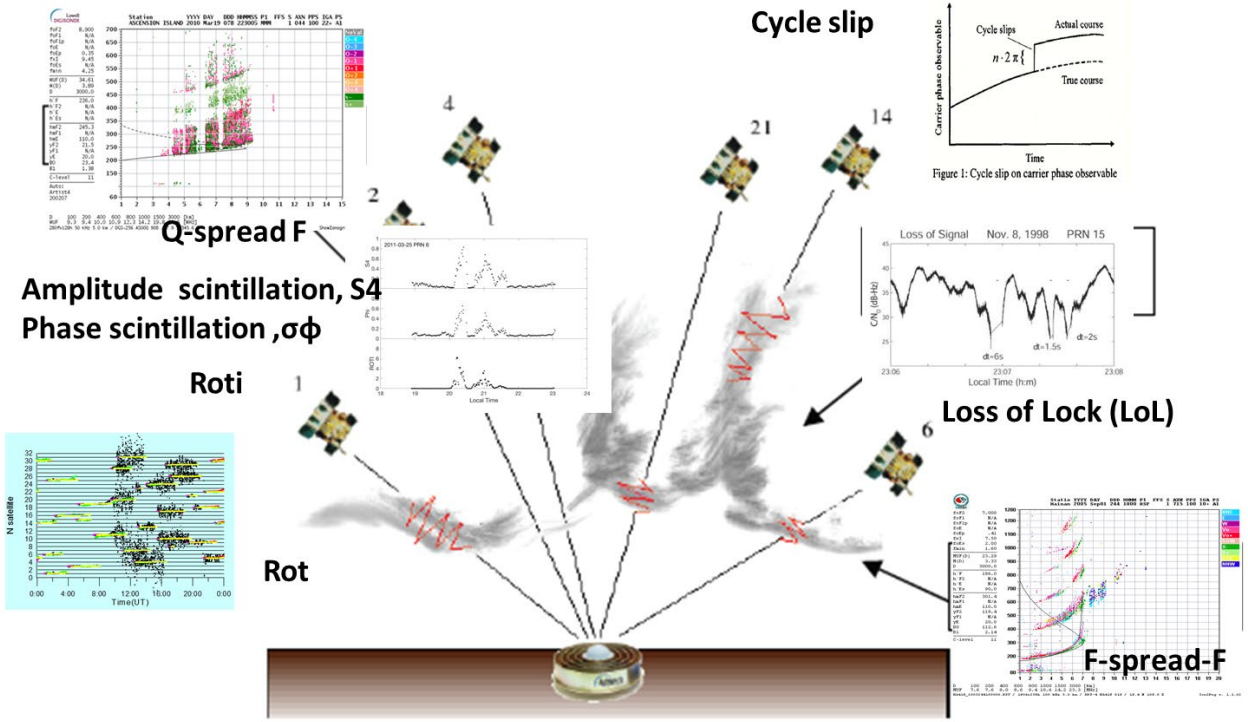

(Courtesy of SBAS Ionospheric Working Group, 2010)

From 1990s, the parameters for describing ionospheric scintillation features mainly derived from GNSS observations

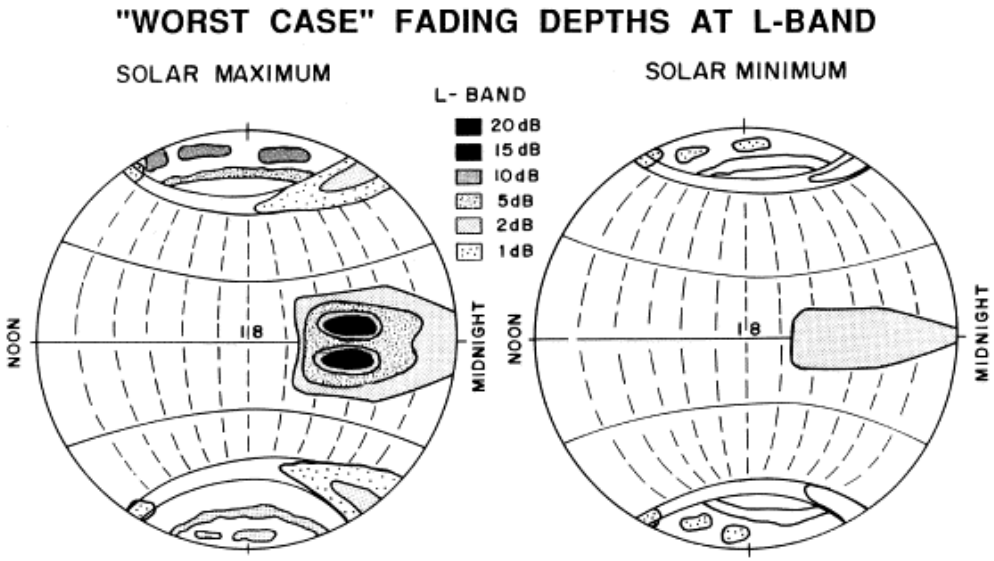

Basu et al., 1988

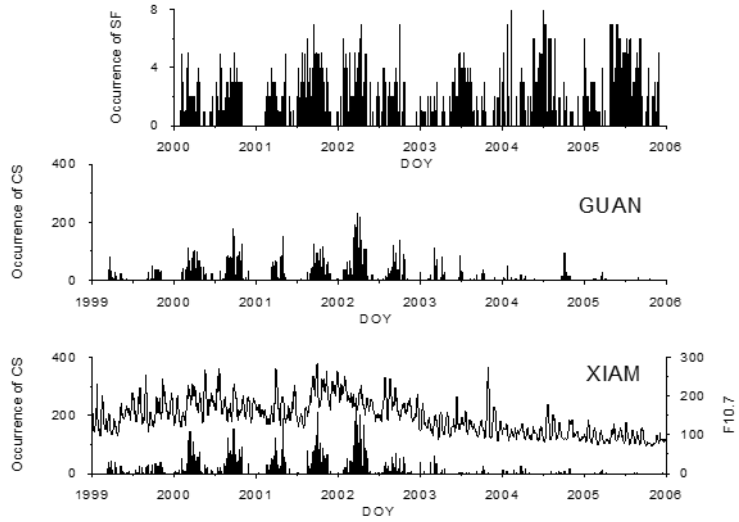

Zhang et al., 2010, cycle slip

Background: Example of the difference to reveal the variation of irregularities or scintillation from different parameters

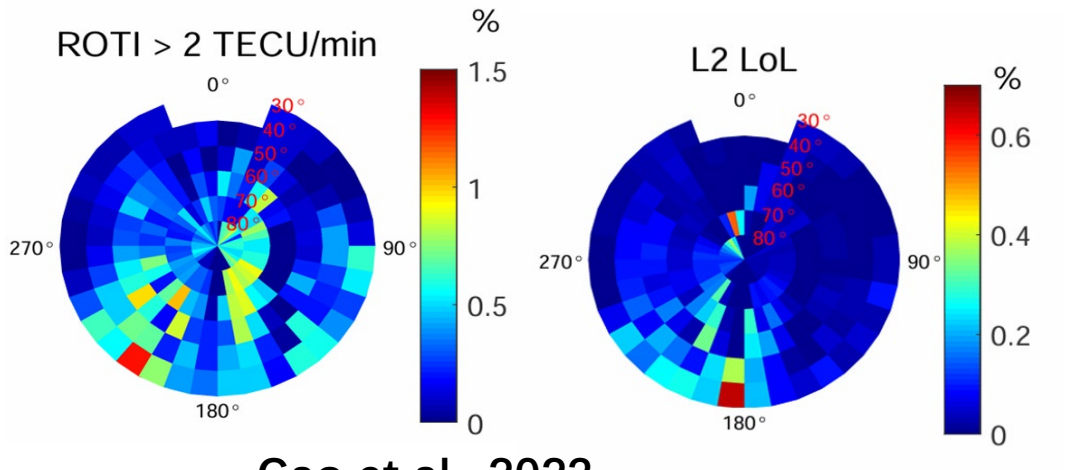

Gao et al., 2023

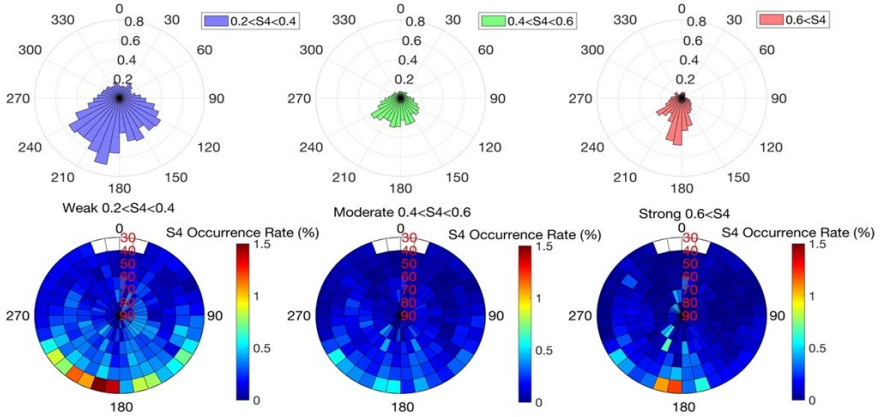

S4 classified with different strength

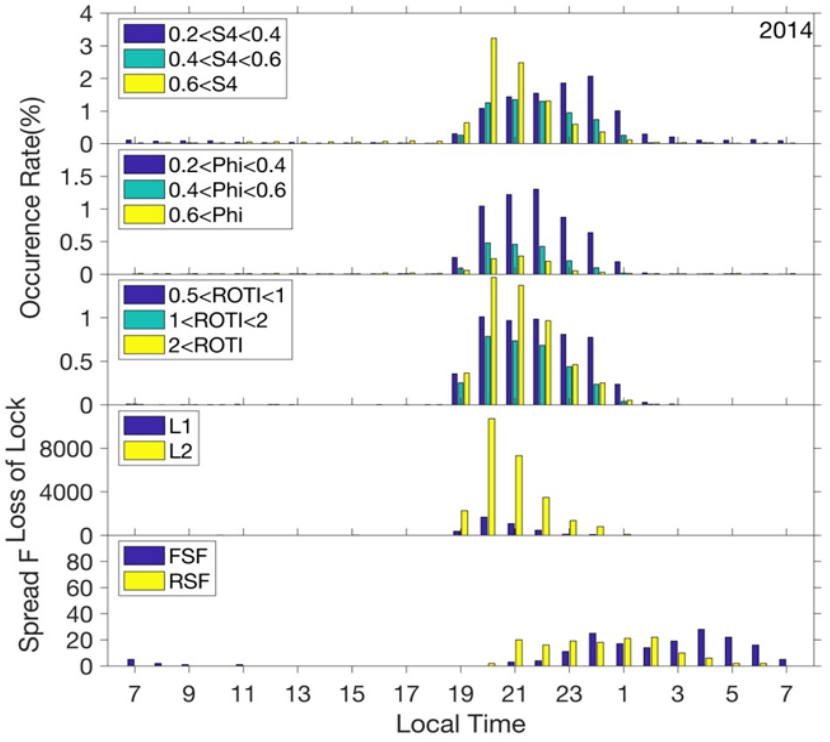

Current understanding about the characteristics of ionospheric irregularities/scintillation usually depend on the different effects of ionospheric irregular structures on radio wave signals, but these effects are not accordant sometimes in detail.

Background： Irregularities and Positioning accuracy

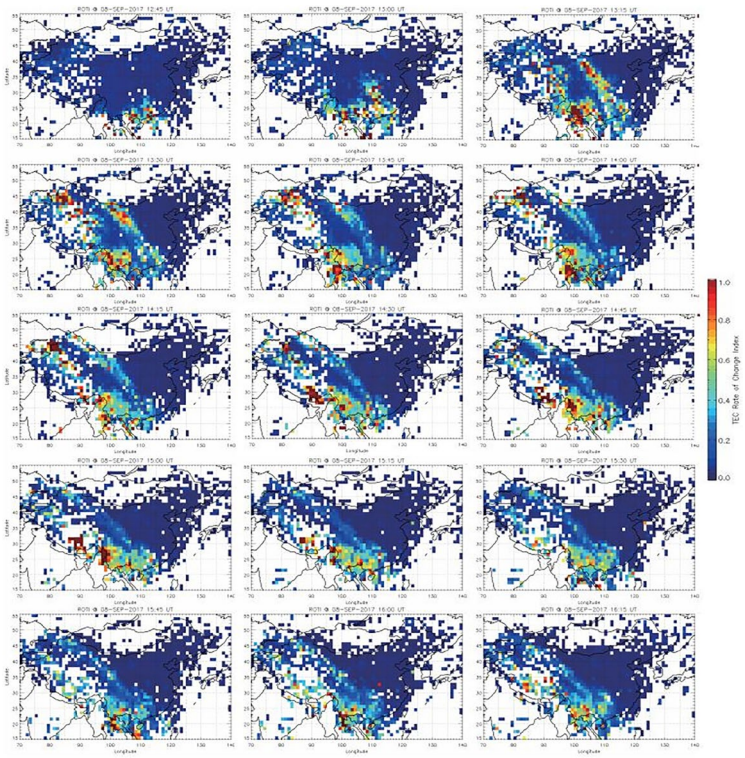

ROTI Map

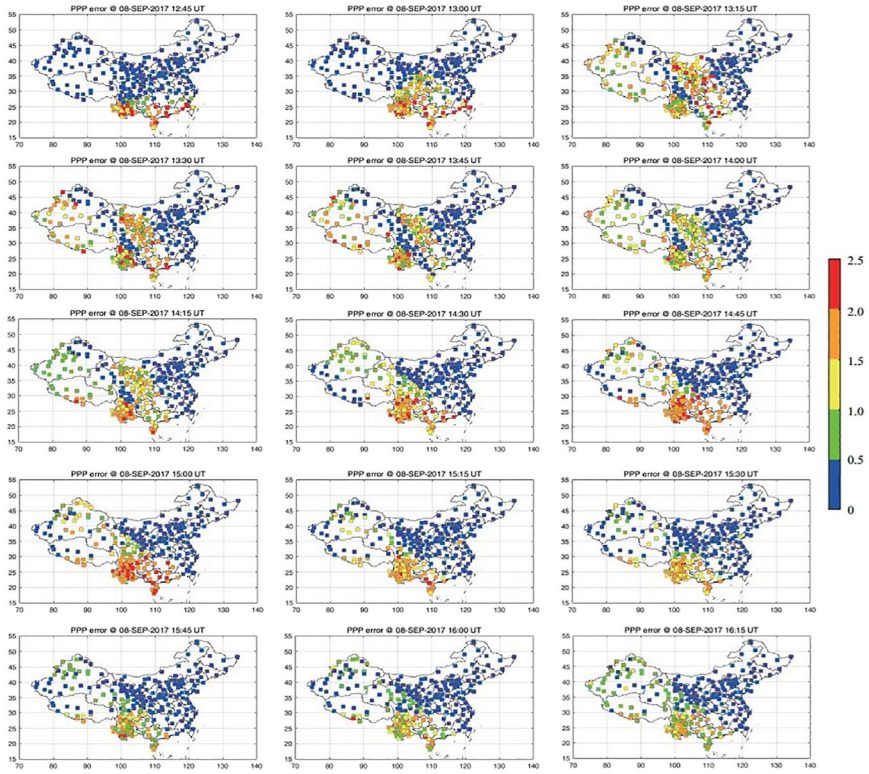

PPP error using RTKLIB PPP

Compared to the space weather effect on the GNSS carrier signal, people are more interested and easy understanding in space weather impact on GNSS positioning accuracy

September, 9, 2017 Storm，Geng et al., 2022

Questions

- **The consistency and differences** of the ionospheric irregularity/scintillation parameters to reveal the morphological variation.
- Although it is widely accepted that ionospheric scintillation can affect the quality of GNSS observations, **the error level and factors influencing GNSS positioning accuracy** should be analyzed in detail.

Motivation

- Showing the consistency and difference of the irregularities distribution with different parameters
- Giving the impact of the ionospheric irregularities on PPP accuracy, carrier signal during storm and analyzing the key factors affecting PPP accuracy.

Data and Mehod

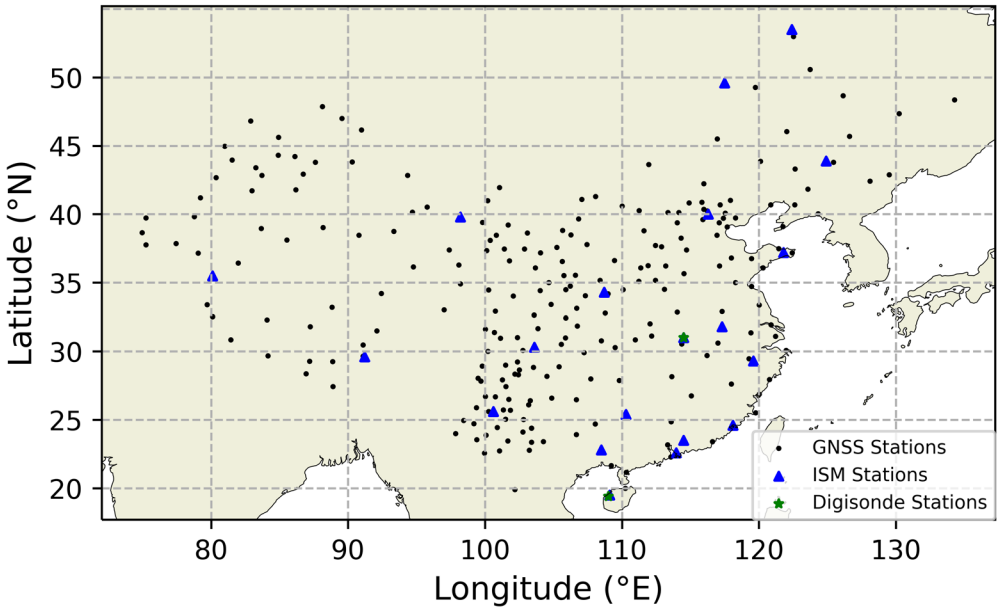

Data

- ~250 GNSS receivers from CMONOC （Trimble, Netr 8, Netr 9)

ROTI、Loss of Lock、 SNR， and PPP error

- 18 ISMRs from China Meridian Project (CMP)

S4（elevation>30°）

- Ionosonde from CMP

Ionograms （Q type SF）

MENU

Canada.ca > Natural Resources Canada > Maps, Tools and Publications > Geodetic Reference Systems > Geodetic tools and data > Precise Point Positioning

Notice: The Canadian Geodetic Survey (CGS) is releasing a new version of NAD83(CSRS) and a new velocity grid NAD83(CSRS) v8 - NAD83v80VG

Precise Point Positioning

CSRS-PPP update – ITRF2020/IGS20 Reference Frame Adoption

Beginning with GNSS observations collected on **Sunday, 27 November 2022**, CSRS-PPP will output ITRF solutions in the IGS20 reference frame. This new frame is the International GNSS Service (IGS) realization of ITRF2020. To learn more about this change and what the impacts may be on your submissions, please visit the CSRS-PPP modernization page.

CSRS-PPP service upgrade from version 2 to version 3

On **Tuesday, 20 October 2020 at 11:00 EDT**, the Canadian Geodetic Survey of Natural Resources Canada updated the Canadian Spatial Reference System Precise Point Positioning (CSRS-PPP) service. This CSRS-PPP modernization includes PPP with ambiguity resolution (PPP-AR) for **data collected on or after 1 January 2018**. Data collected prior to this date will continue to be processed with the IGS final products without ambiguity resolution. For more information, please visit the CSRS-PPP modernization page or download the tutorial describing the changes.

Item	Strategies
Interval	30s
Elevation angle cut-off	7.5°
PPP processing model	Kinematic
GNSS system	GPS
Function model	Uncombined model
Frequency	Double
Observations	Pseudorange and carrier phase
Vertical datum	CGVD2013
Reference system	ITRF2020
Filter type	Forward and backward
Troposphere model	VMF1
Orbit and clock state	IGS products(sp3;clk)
Satellite antenna files	IGS20.atx
Parameter estimation	Sequential normal stacking
Ambiguity validation	Weighted integer decision

PPP Positioning algorithm:
CSRS-PPP (on line)

Error of three coordinate components 3D error

$$3D_{error} = \sqrt{dx^2 + dy^2 + dz^2}$$

Number of tracked satellite and GDOP (Geometric dilution of precision) with elevation >7.5 degree

Space environment condition during Storm on Dec. 1, 2023

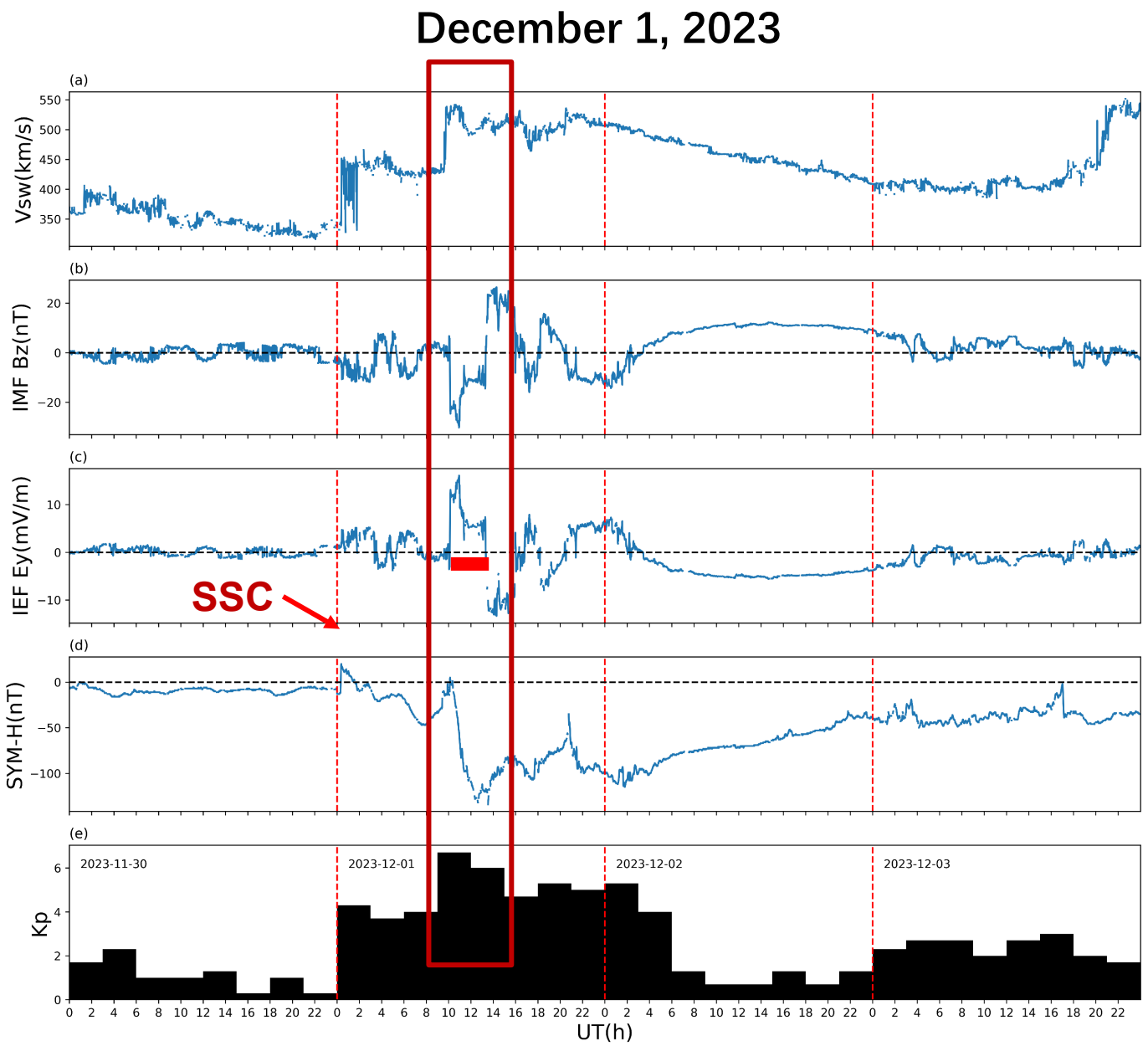

Solar wind suddenly increased from 320 to 450 km/s at 0: 30 UT. After lasting about 9 hours. It suddenly increased to~540 km/s at 09:40 UT

Then, IMF Bz turn southward and lasting about 3.5 hrs

In the meantime, IEy turns eastwards lasting 3.5 hrs (local time :18:00 tp 22:00)

Minimum SYM-H: -132 nT at about 13 UT

Maximum Kp: 7

Result: ROTI, SNR, S4 from low to middle latitude receivers during the storm

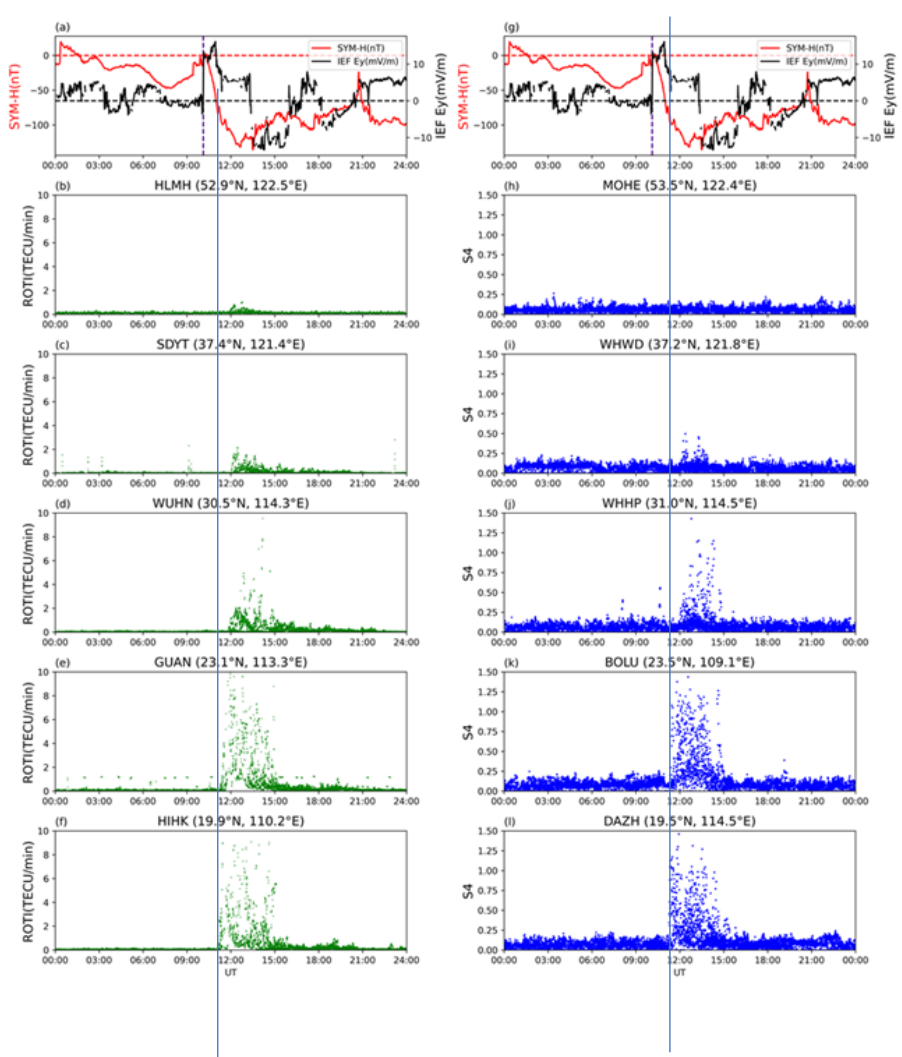

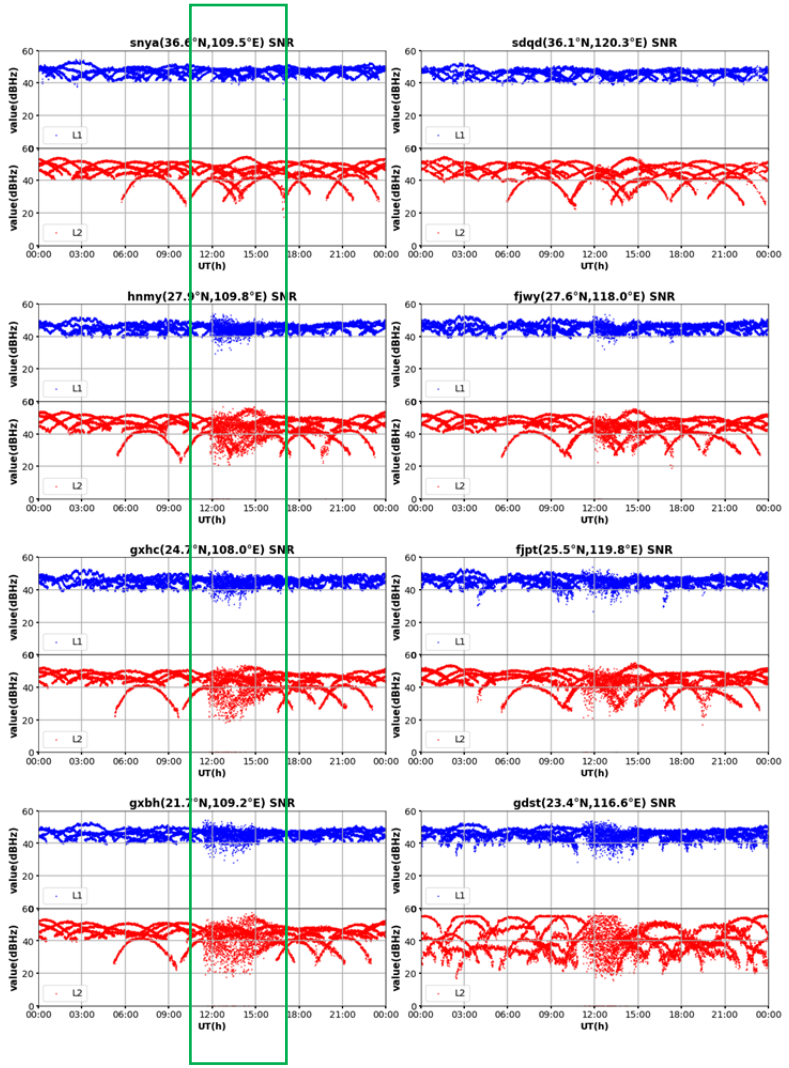

The scintillation occurred, and its strength decreased from low to middle latitude showed in ROTI, S4 index
The quick fluctuation of SNR (signal fading) in L1 and L2 occurred during storm, L2>L1

The beginning time of scintillation: low latitude at about 11: 40 UT, middle latitude 12: 00 UT

ROTI

S4

SNR in L1 (Blue) and L2 (red) carrier signal

Result: Ionogram at Danzhou and Wuhan

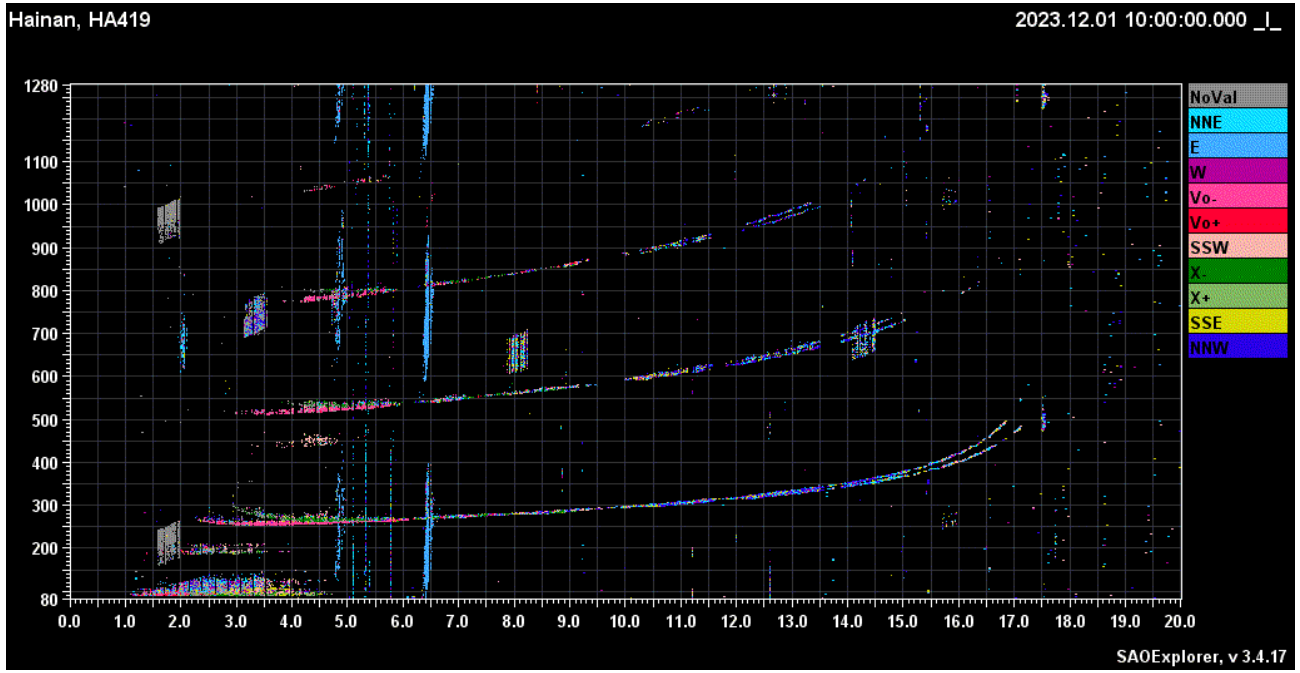

Danzhou, Hainan

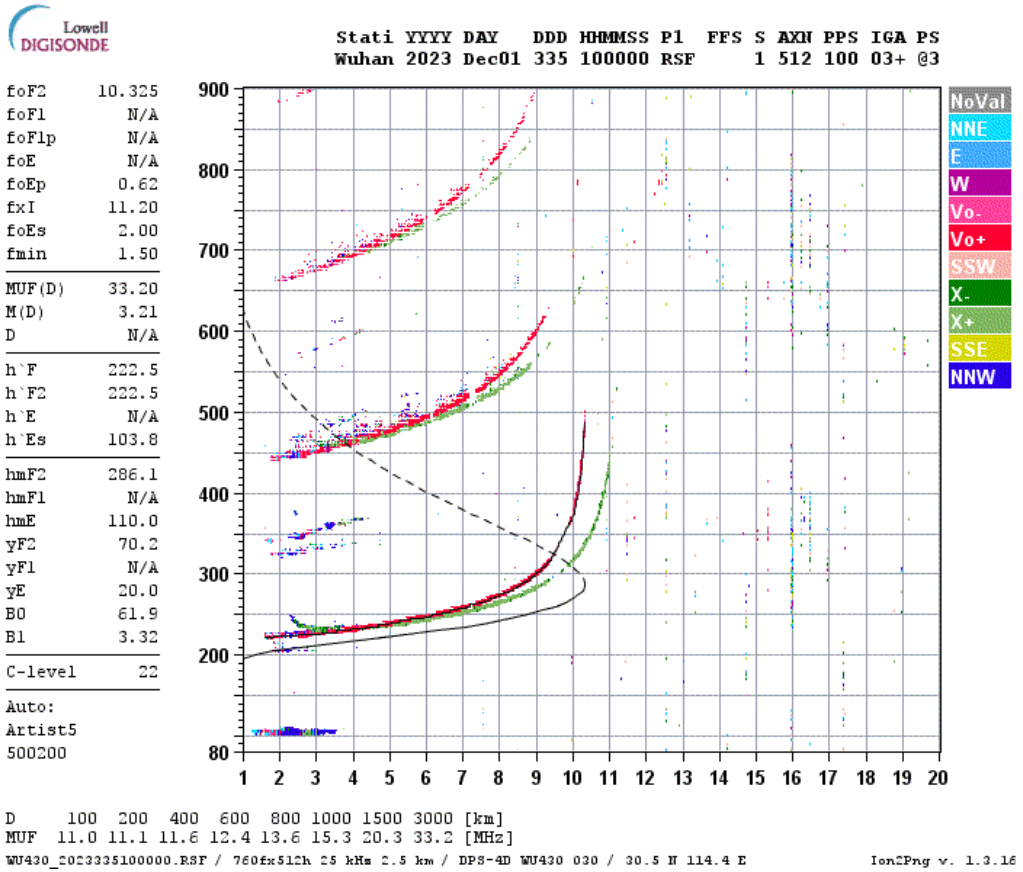

Wuhan, Hubei

Strong Q type SF in 20 N (stronger Hainan) and 30 N (Wuhan)

Result: Spatial and temporal distribution of ROTI, LoL and S4 value

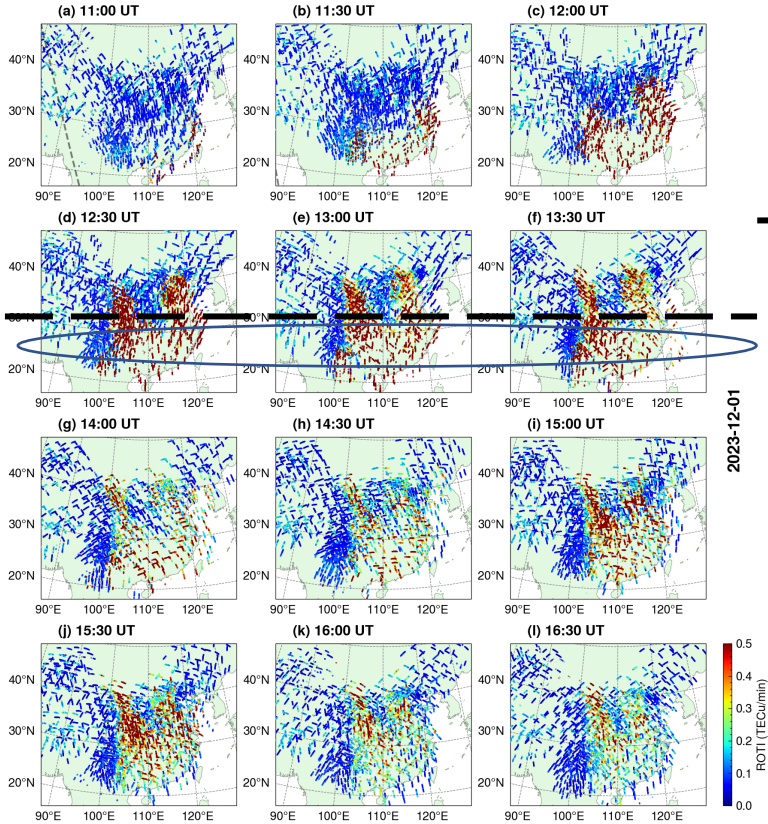

ROTI maps from CMONOC with continuous time interval (30 min)

ROTI: 12 -13:30 UT from 10 do 40 N, shows two structure in middle latitude (east and west) along northwest direction, sparse data in part of low latitude.

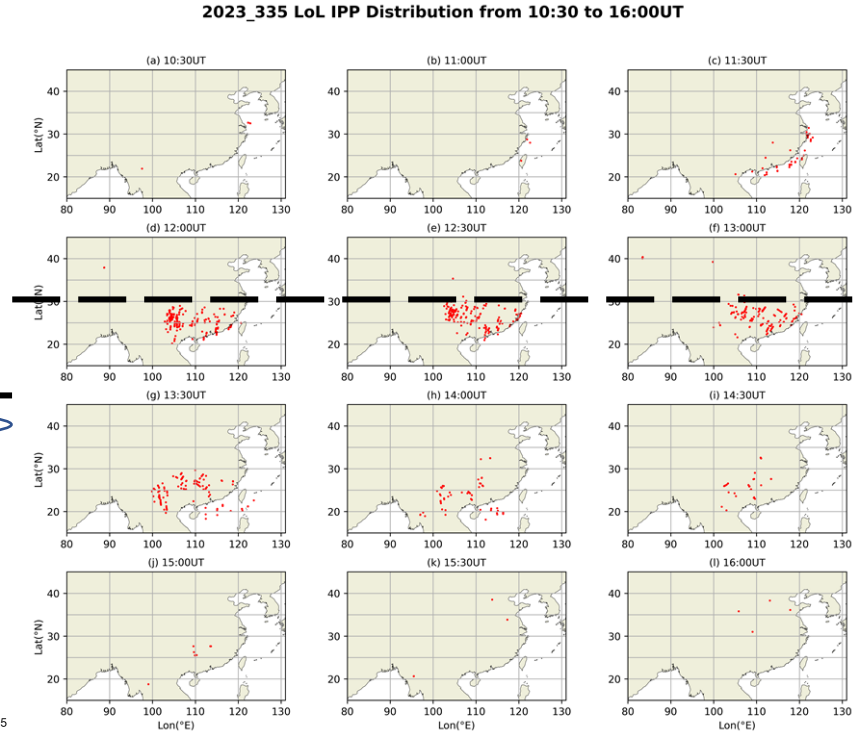

Spatial Distribution of IPP of LoL from CMONOC receivers with 30 min interval

LoL: Occurred less 30 N, peak period 12-13 UT

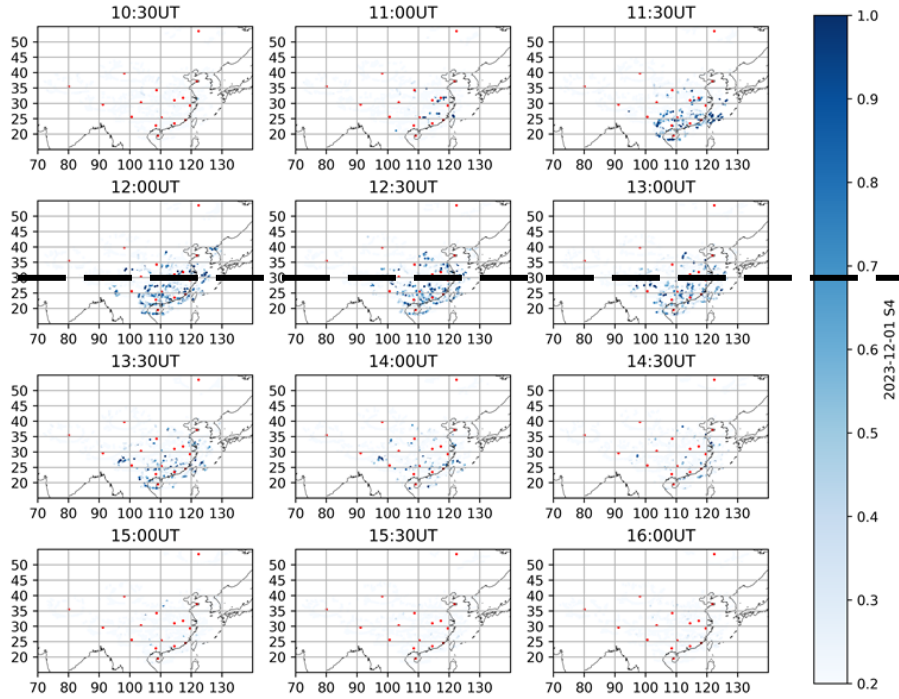

Spatial distribution of S4 (L1 signal) values from 14 ISMR at different interval (all GNSS signal)

S4: peak period 12-13 UT, stronger in the latitude < 30 N

Results: Impact on CMONOC GNSS PPP accuracy

北京大学 PEKING UNIVERSITY

Affected

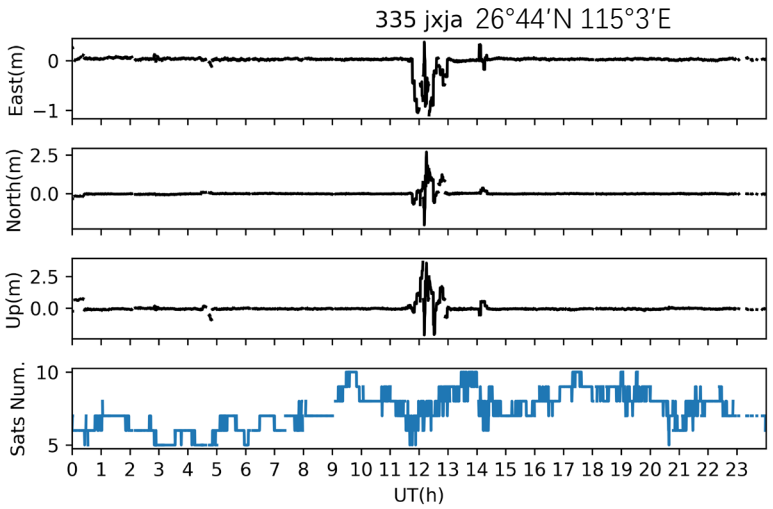

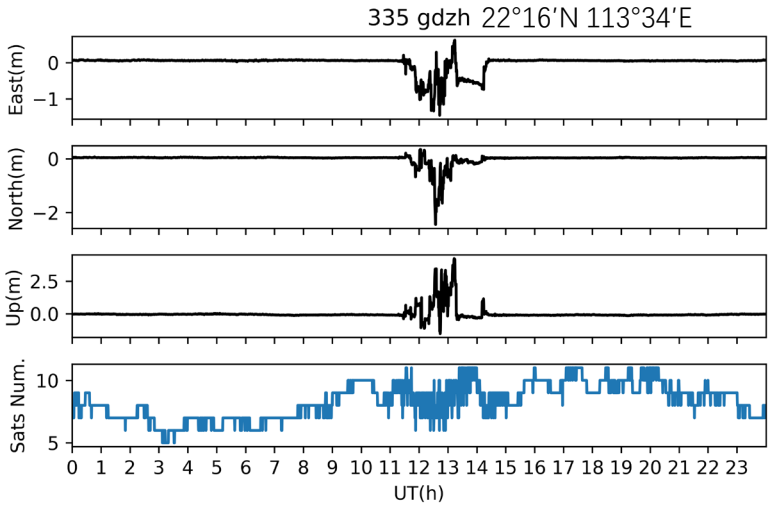

No affected

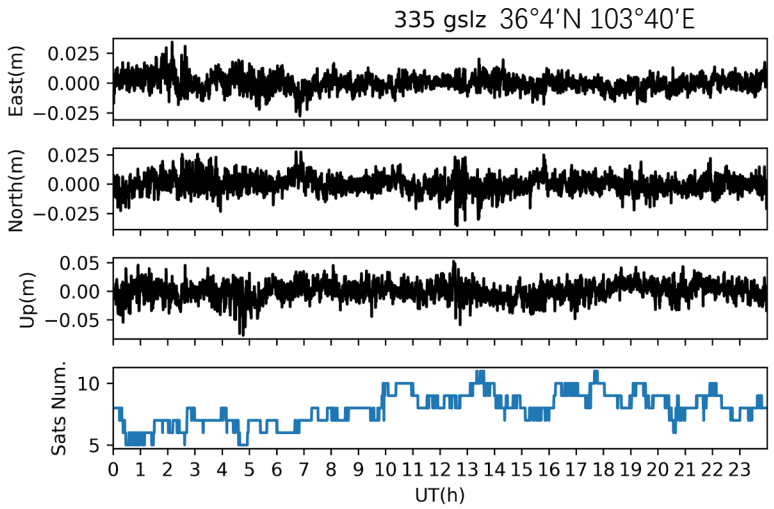

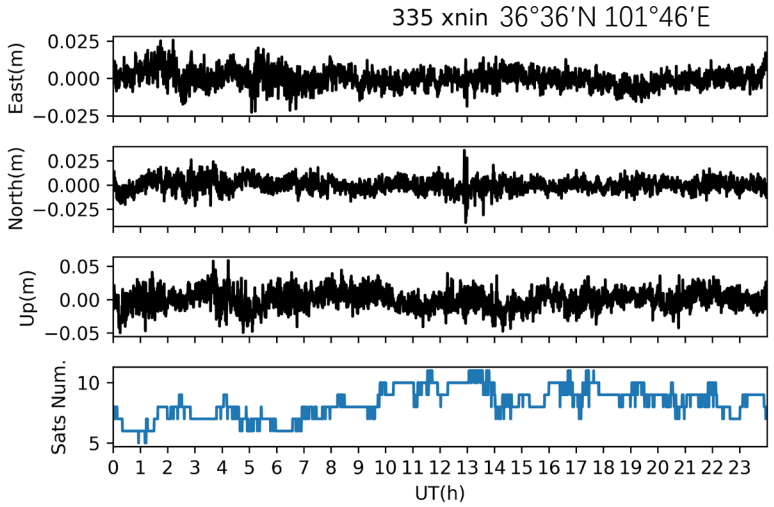

Three coordinates components (east, north and up) from 4 GNSS station (kinetic CSRS- PPP)

Affected

Errors 1-3 m
Lasting time about 3 hours

No affected
Average error:3-5 cm

Results: Scattergram of the Impact on CMONOC GNSS PPP accuracy

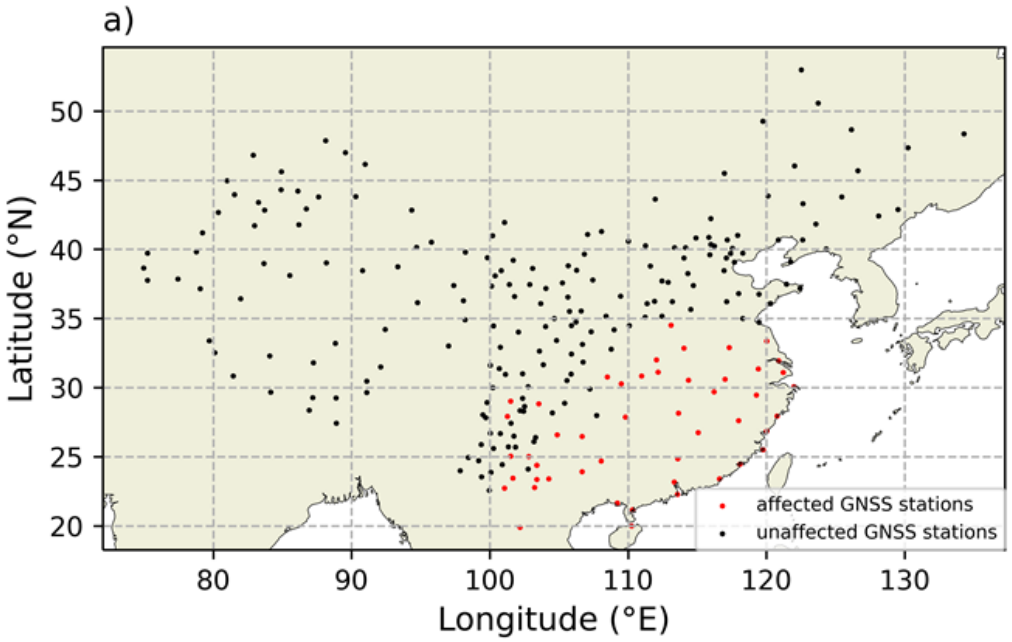

The distribution of affected stations (red dot) and unaffected stations (black dot)

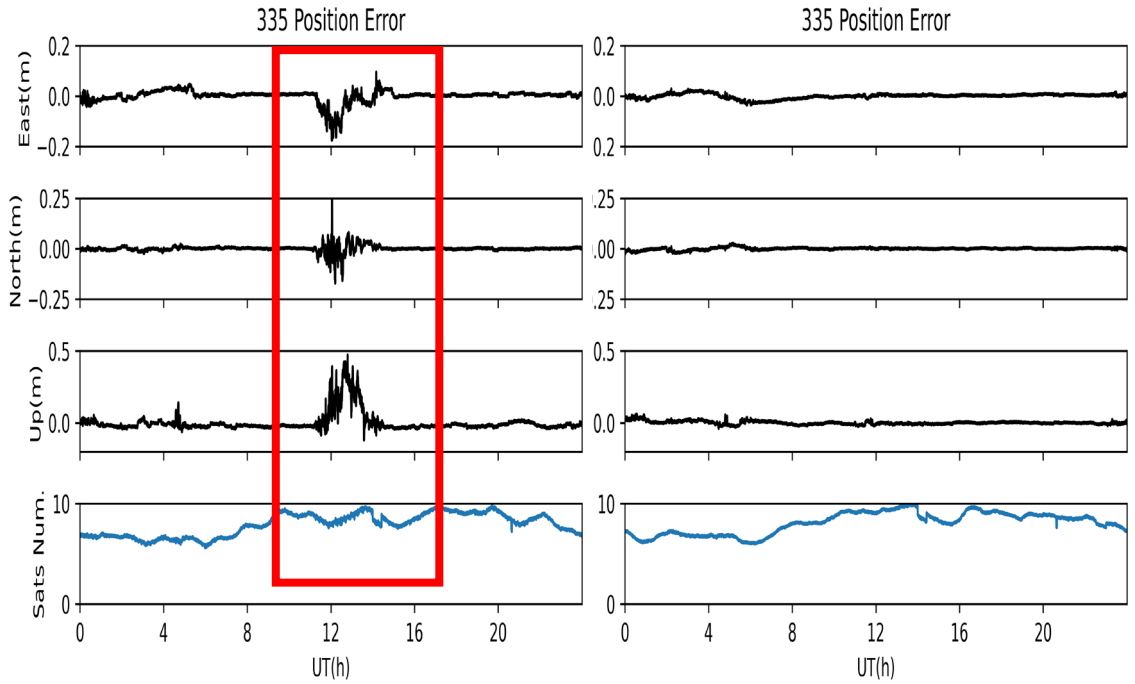

Positioning errors and the number tracked satellite averaged all affected stations

Averaged for all unaffected stations

Result: Distribution of PPP 3-D Error and the total number of LoL from each receiver during continuous time interval

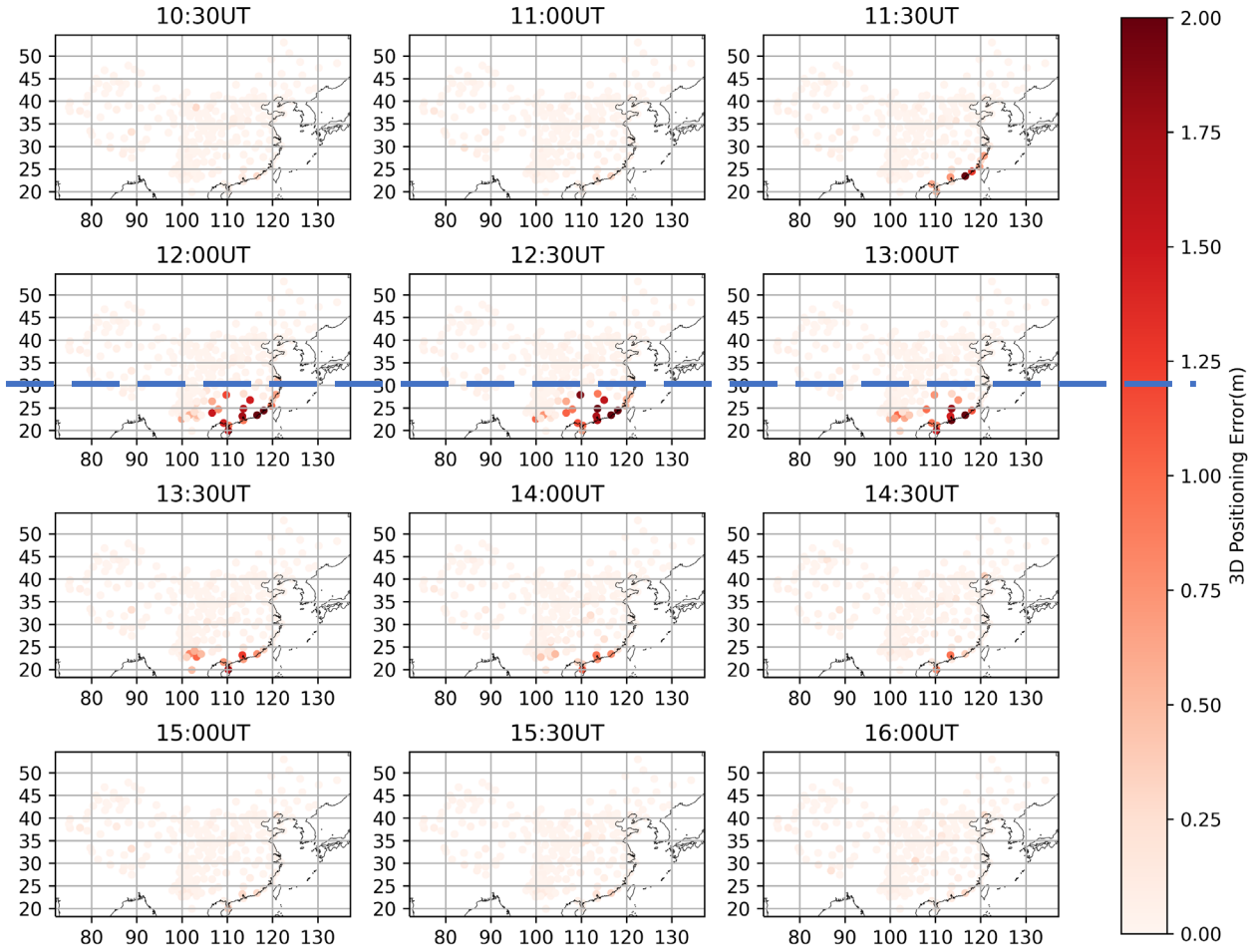

Distribution of 3-D error average from each receiver during continuous 30-minute intervals

$$3D_{error} = \sqrt{dx^2 + dy^2 + dz^2}$$

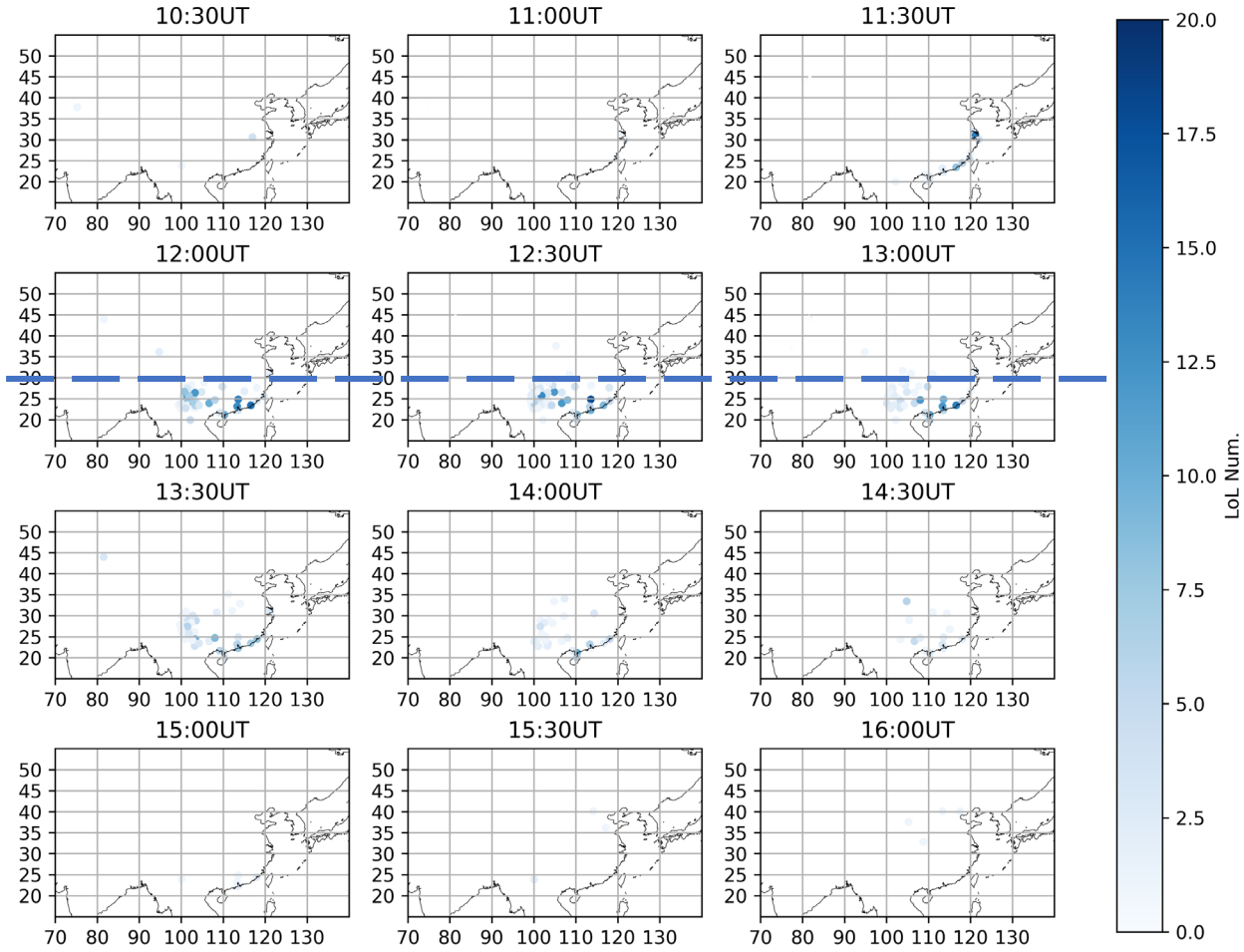

Distribution of total number of LoL from each receiver during continuous 30-minute intervals

Discussion

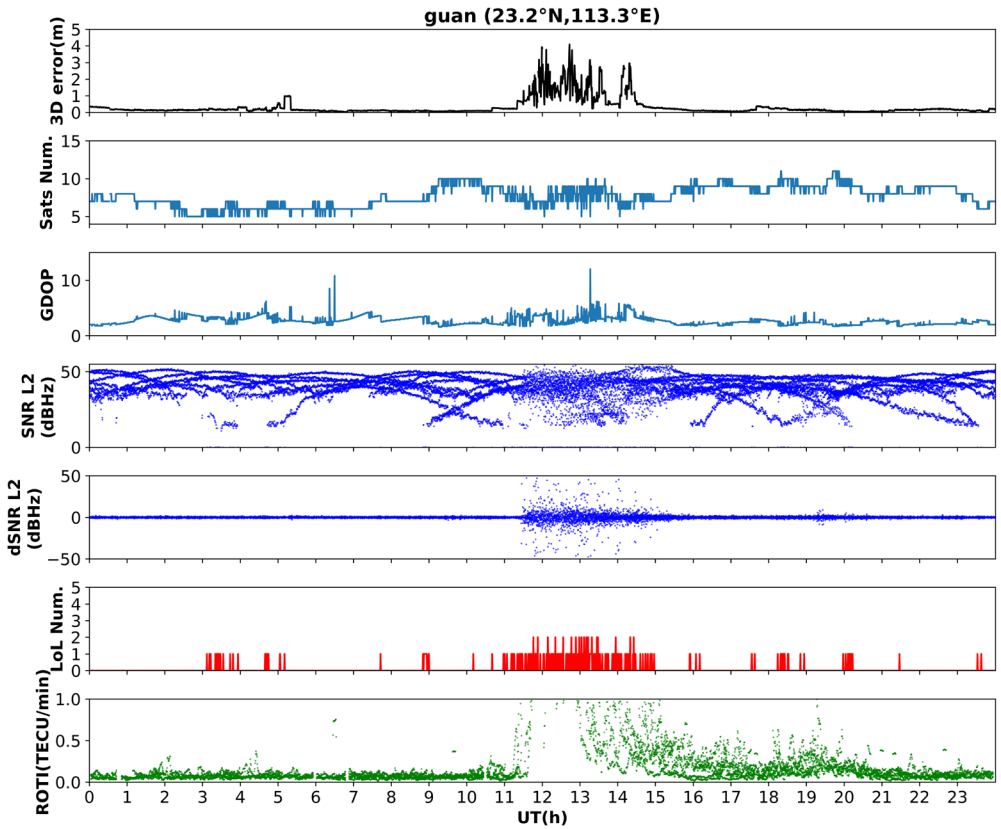

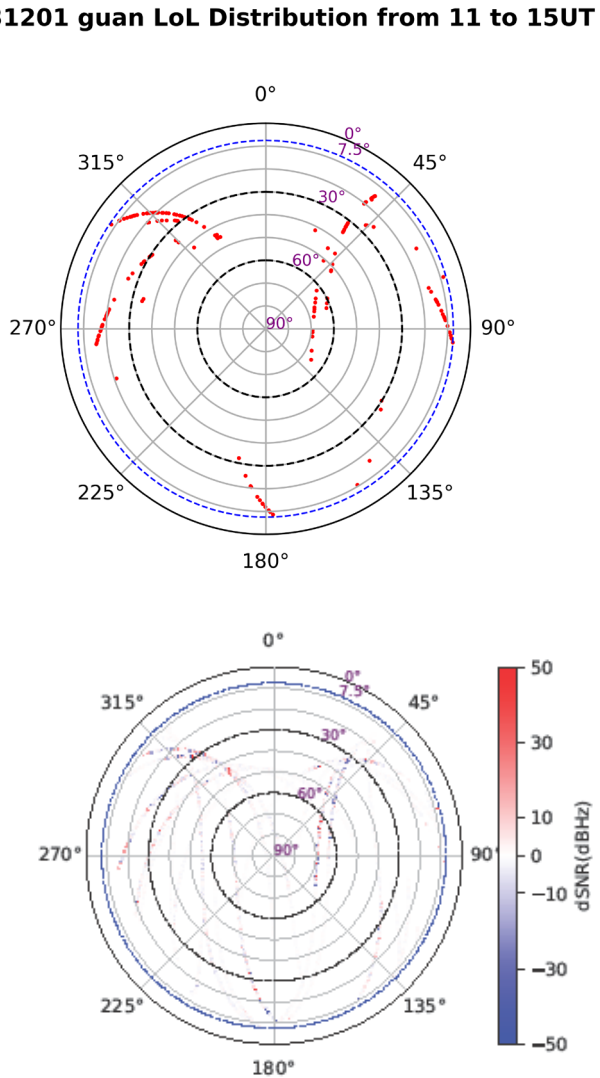

LoL increase GDOP value that is calculated from geometrical distribution of tracked satellites

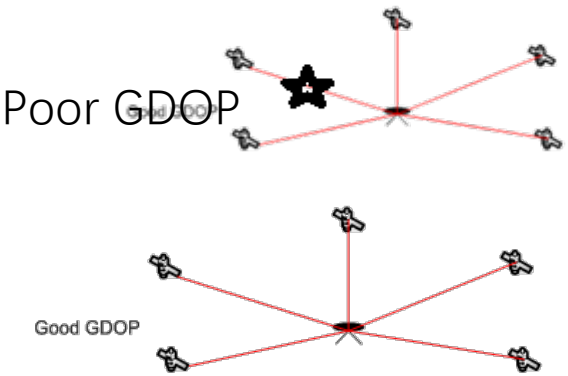

The quick and large fluctuation of SNR may affect the key process to determination of ambiguity resolution and ambiguity evaluation in PPP algorithm.

Summary

- During geomagnetic storms, multiple ionospheric scintillation parameters exhibit significant fluctuations, indicating the presence of ionospheric irregularities. However, there are slight differences among these parameters in characterizing the spatiotemporal distribution of ionospheric scintillation.
- During geomagnetic storms, the occurrence of ionospheric scintillation leads to an increase in the average PPP positioning error across China. Compared to higher-latitude regions, the lower-latitude areas experience earlier onset of positioning error disturbances, longer persistence, and greater error magnitudes, with the maximum 3D error reaching approximately 1 meter.
- The distribution and evolution trend of dynamic PPP errors are similar to the pattern of the LoL index, with regions exhibiting higher LoL counts generally demonstrating elevated dynamic PPP errors compared to quiet regions.
- The impacts of loss-of-lock and positioning errors are primarily observed below 30° N, whereas multi-parameter observations indicate that irregularities can extend to around 40° N.

Zeng, Y., Zhang, D., Li, K., Tian, Y., & Yang, G. (2026). The evolution of the ionospheric irregularities and their effects on GNSS over China during the geomagnetic storm on 1 December 2023. Space Weather, 24, e2025SW004882. https://doi.org/10.1029/2025SW004882

Thanks for your attention!

谢　谢（XieXie）